ELSEVIER

Tectonophysics 333 (2001) 123–134

TECTONOPHYSICS

www.elsevier.com/locate/tecto

An alternative interpretation for slip vector residuals of subduction interface earthquakes: a case study in the westernmost Ryukyu slab

Ling-Yun Chiao[a,*], Honn Kao[b], Serge Lallemand[c], Char-Shine Liu[a]

[a]*Institute of Oceanography, National Taiwan University, Taipei, Taiwan, ROC*
[b]*Institute of Earth Sciences, Academia Sinica, Taipei, Taiwan, ROC*
[c]*UMR CNRS-UM2 5573, Laboratoire de Geophysique et Tectonique, ISTEEM, Montpellier, France*

Abstract

Slip partitioning along oblique subduction zones has conventionally been examined by slip vector residuals determined from interface earthquakes. It is measured through contrasting the slip vector with respect to the local plate convergence direction defined on the surface of the Earth by the Euler vector. Interpretation of regional plate kinematics based on slip vector residuals thus defined may be misleading. Besides the apparent discrepancy attributable to the surface projection of vectors on an obliquely plunging surface, a more fundamental problem is the construction of the reference subduction flow field for the subducted slab based upon the known plate convergence. It can be shown that for complicated slab geometry, the conventional practice of intuitively rotating the Euler kinematics onto the subducted slab leads to unrealistic intraplate deformation that invalidates the mechanical integrity of the oceanic lithosphere. Alternatively, we propose to calculate the velocity field for the specific slab geometry based on the rationale that the subduction flow field should be the one that endures the least amount of intraplate deformation. The calculated flow field for the westernmost Ryukyu slab, that is in transition to the Philippine Sea plate (PSP)–Eurasian Plate (EP) collision near Taiwan, reveals quite distinct subduction flow field. The particle paths associated with the calculated flow field are in better accordance with the observed slip vectors while the corresponding strain-rate field is consistent with the previously reported lateral compression seismogenic zone. Furthermore, it is speculated that the plate kinematics of the northwestern corner of PSP that is impinging the vicinity of the collision might have also undergone significant readjustment to accommodate the potential intraplate deformation. It is noted that the westernmost subducted Ryukyu slab and the northwestern corner of PSP belong to a mechanically coherent tectonic unit. The 3D geometric constraints set up by the subducted slab and the "unfriendly" kinematic constraints imposed by the collision boundary both play important roles in configuring the intraplate deformation within PSP. Manifestation in the local kinematics might indicate deviation from the general PSP–EP convergence, and is thus of crucial importance to tectonic interpretations of geophysical observations in this area.

Keywords: slip vector residual; intraplate deformation; minimum deformation rate kinematics

1. Introduction

The majority of earthquakes in subduction zones occur along the plate interface. Slip vectors determined from source parameters of these interplate earthquakes have been invoked as important kinematic constraints in the study of regional plate tectonics. The usual convention used to describe the slip vector with respect to the local plate kinematics consists of the convergence obliquity (ϕ_{OBL}) and the

* Corresponding author. Tel: +886-2-2362-2875; fax: +886-2-2362-6092.
E-mail address: chiao@ccms.ntu.edu.tw (L.-Y. Chiao).

0040-1951/01/$ - see front matter
PII: S0040-1951(00)00271-7

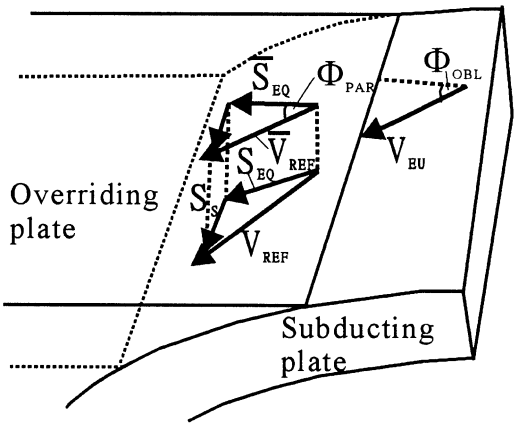

Fig. 1. Schematic diagram illustrating the "slip partitioning". $\mathbf{V}_{EU}$ is the Euler kinematics representing the plate convergence on the surface of the Earth. The convergence obliquity, ϕ_{OBL}, is defined by the angle subtended by $\mathbf{V}_{EU}$ with the local trench normal. On the inclined plate interface, slip vector of an interface earthquake is $\mathbf{S}_{EQ}$, while the reference subduction flow field at the same location is $\mathbf{V}_{REF}$. A deviation ($\mathbf{S}_S = \mathbf{V}_{REF} - \mathbf{S}_{EQ}$) indicates that there exists additional relative motion between the subducted slab and the overriding plate. Let slip obliquity ψ (not shown here) be the angle between the surface projection of the slip vector ($\bar{\mathbf{S}}_{EQ}$) and the trench normal, the "slip vector residual" is defined by the difference $\phi_{PAR} = \phi_{OBL} - \psi$. Notice that this definition assumes that the direction of the surface projection of the subduction flow field ($\bar{\mathbf{V}}_{REF}$) is consistent with $\mathbf{V}_{EU}$ at the epicenter of the interface earthquake.

slip obliquity (ψ) (Fig. 1). For plate convergence defined by the Euler vector ($\mathbf{V}_{EU}$), ϕ_{OBL} is defined by the angle subtended by $\mathbf{V}_{EU}$ with the local trench normal, whereas ψ is defined as the angle between the surface projection of the slip vector and the trench normal. The difference ($\phi_{PAR} = \phi_{OBL} - \psi$) is sometimes referred as the "slip vector residual" (McCaffrey, 1992), and the ratio ϕ_{PAR}/ϕ_{OBL} has been defined as the so-called " degree of slip partitioning" (Liu et al., 1995). For the naïve scenario with normal plate convergence across the trench ($\phi_{OBL} = 0^{\circ}$), the surface projection of the slip vector is usually consistent with the Euler vector, and there will thus be no slip vector residual. However, for significant convergence obliquity, that is, ϕ_{OBL} greater than the critical threshold (McCaffrey, 1992; Liu et al., 1995), noticeable slip partitioning has been reported and attributed to arc-parallel shearing of the fore-arc sliver (e.g. Fitch, 1972; McCaffrey, 1992, 1993, 1994; Lallemand et al., 1999b). Liu et al. (1995), on the other hand, proposed to relax the rigidity requirement of the subducted slab and attribute the cause of slip vector residuals to the slab deformation induced by the dynamical gravitational pulling.

From a strictly kinematic point of view, the implication of interest from observations of interplate slip vectors on the local tectonics stems from examining the possible decoupling of the plate convergence vector into both the strike–slip and the dip–slip components along the inclined plate interface. As shown in Fig. 1, if the reference frame is fixed onto the overriding plate, the plate convergence on the inclined plate interface is represented by the subduction flow field ($\mathbf{V}_{REF}$) whereas the slip vector along the inclined plate interface is $\mathbf{S}_{EQ}$. A deviation ($\mathbf{S}_S = \mathbf{V}_{REF} - \mathbf{S}_{EQ}$) indicates that there exists additional relative motion between the subducted slab and the overriding plate, such as the arc-parallel shearing of the fore-arc sliver. However, slip partitioning described above is measured by the deviation on the surface of the Earth ($\bar{\mathbf{V}}_{REF}$ is the surface projection of $\mathbf{V}_{REF}$ and $\bar{\mathbf{S}}_{EQ}$ is projected from $\mathbf{S}_{EQ}$ in Fig. 1). There is an apparent discrepancy resulting from the projection, namely, deviation between vectors on an inclined interface will be underestimated after being projected to the surface of the Earth. Fortunately, this effect is usually minor for a shallowly dipping plane. A more fundamental controversy, however, is the implicit assumption that $\bar{\mathbf{V}}_{REF}$ is consistent with the local $\mathbf{V}_{EU}$, that is, the local Euler vector defined on the surface of the Earth. A better construction of $\mathbf{V}_{REF}$ from $\mathbf{V}_{EU}$, based on the assumption that there are only simple bending deformations across the trench, characterizes the subduction flow field by simply rotating the Euler kinematics with respect to the local trench axis through the dip angle. However, it has been reported that for several subduction zones, significant lateral membrane deformations are required to achieve the observed slab geometry (Burback and Frolich, 1986; Yamaoka et al., 1986; Creager and Boyd, 1991). The intuitive flow field of the subducted slab, constructed by simply rotating the reference Euler kinematics, usually leads to unrealistic intraplate deformation that invalidates the mechanical integrity of the oceanic lithosphere. Alternatively, it is possible to calculate the velocity field for the specific slab geometry based on the rationale that the subducted flow field should be the one that endure

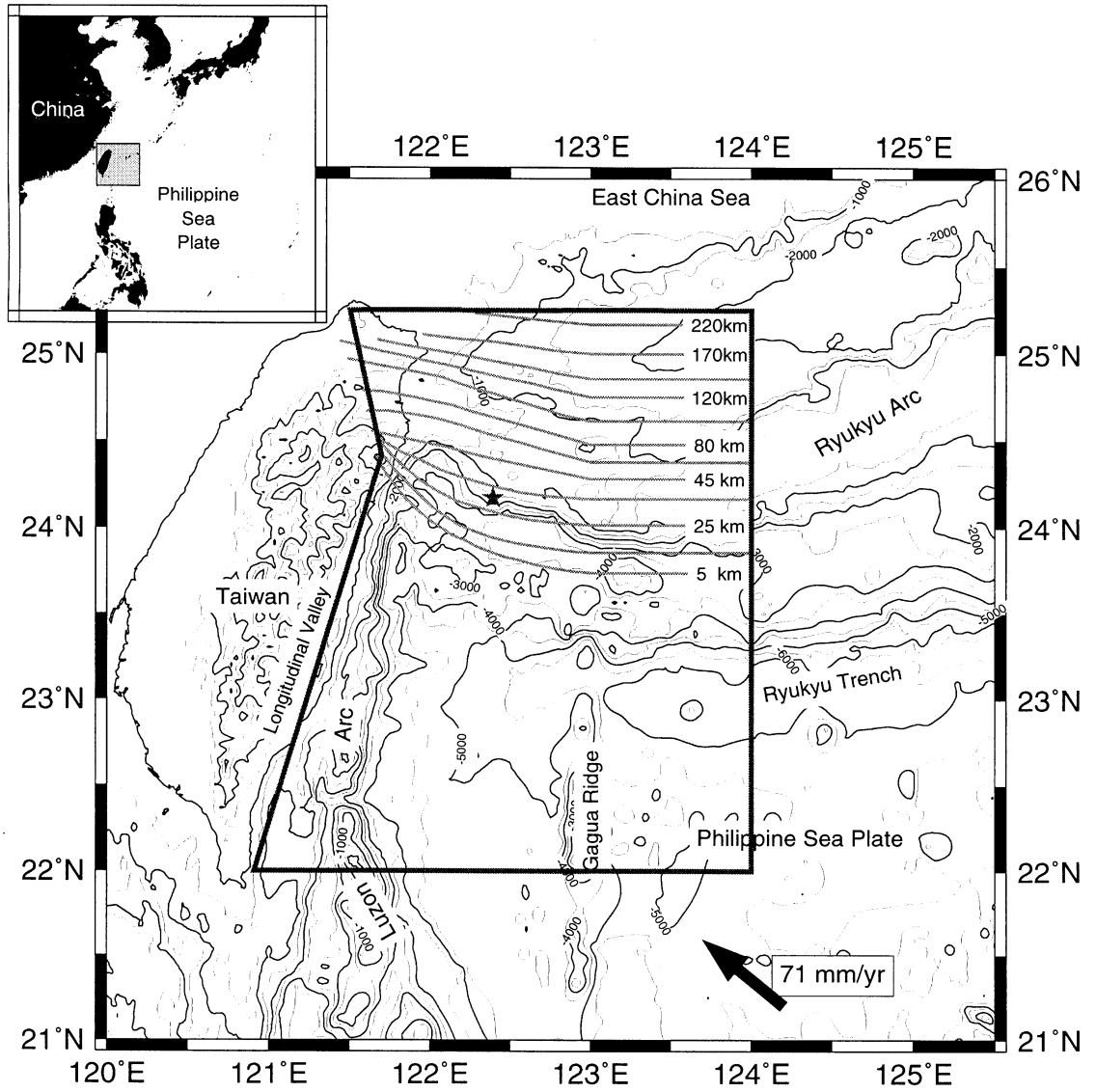

Fig. 2. Tectonic background of the northwestern corner of PSP and the westernmost subducted Ryukyu slab. The bold frame marks our modeling region. Bathymetric contours are in 500 m contour interval. Light gray contours of slab geometry inferred from slab seismicity are, respectively, depths of 5, 15, 25, 35, 45, 60, 80, 100, 120, 140, 170, 220 km (after Kao et al., 1998a). Grey star near 24°N, 122.5°E marks the location where a patch of interface earthquakes with noted slip vector residuals are observed. Solid arrow indicates the average PSP–EP convergence (Seno et al., 1993) in this area.

the least amount of intraplate deformation (Creager and Boyd, 1991; Chiao, 1993). The calculated velocity vector field can then be served as the reference field for the purpose of examining slip vector residuals for interface earthquakes.

In this study, we focus our efforts to the westernmost Ryukyu arc where a 70° convergence obliquity and average slip vector residual of 35° are reported (Fig. 2, Kao et al., 1998a). However, many recent observations, including earthquake focal mechanisms,

detailed bathymetry, seismic profiling, and GPS measurements, suggest that there is no corresponding large-scale shear structure in the overriding plate at sites close to the observed interface events (Lallemand et al., 1999a). The purpose of this study is thus to investigate the kinematics characteristic of the northwestern corner of the Philippine Sea Plate (PSP), including the subducted westernmost Ryukyu slab by numerical modeling. Assuming that the PSP in this region is not strictly rigid (Kao et al., 1998b), we will demonstrate that the systematic distortion of the subducted slab is favored by the region's unique tectonic setting. The significant change of local plate convergence might offer an alternative interpretation of the observed slip vector residuals. Consistencies with other geophysical observations are also examined.

2. Numerical modeling of plate kinematics on a non-Euclidean surface

The fundamental rationale we adopt in this study, which is consistent with plate tectonics, is that the subduction flow field is the one that endures the least amount of intraplate deformation. The first numerically challenging task is the capability of characterizing intraplate deformation in the forward sense. That is, within a modeling region, if the plate kinematic flow field is defined on a non-Euclidean surface composed by the subducting oceanic lithosphere, a numerically tractable scheme to compute intraplate deformation is required. Based on a viscous thin-sheet approximation, the three-dimensional (3D) strain-rate tensor **D** on the given surface can be evaluated by taking the symmetric part of the spatial gradient tensor of the velocity vector field. The intraplate deformation rate, the *in-plane* deformation rate, which includes stretching, compression and shearing taking place within the surface of the slab, can be extracted via the projection operator **P** (Creager and Boyd, 1991; Chiao, 1993):

$$\mathbf{P} = \mathbf{I} - \mathbf{e}_n\mathbf{e}_n^{\mathrm{T}} \tag{1}$$

where e_n is the local unit normal vector perpendicular to the slab surface, $\mathbf{e}_n\mathbf{e}_n^{\mathrm{T}}$ is a dyadic outer product and **I** the identity operator. Operating on **D** by **P** from both sides will annihilate any component of the strain-rate tensor associated with the shear flow outside the slab surface and compression or extension in the slab normal direction. That is:

$$\mathbf{D}^{\mathrm{pp}} = \mathbf{P}\cdot\mathbf{D}\cdot\mathbf{P}^{\mathrm{T}} \tag{2}$$

yields the in-plane strain-rate tensor anywhere on the given 3D surface. To comply with the assumption of incompressibility, we define:

$$\mathbf{D}^{\mathrm{in}} = \mathbf{D}^{\mathrm{pp}} - \mathrm{trace}(\mathbf{D}^{\mathrm{pp}})\cdot\mathbf{e}_n\mathbf{e}_n^{\mathrm{T}} \tag{3}$$

$\mathbf{D}^{\mathrm{in}}$ is thus the strain-rate tensor describing the membrane deformation rate and the thickening or thinning of the viscous slab, or the intraplate deformation we are interested in. Furthermore, if we assume the slab has a power-law viscous rheology in which **D** is proportional to the nth power of the stress, then the dissipation power of the entire flow is proportional to the surface integral over the entire slab of the stress tensor contracted with the strain-rate tensor:

$$I = \int\left\{\sum_{i=3}\left[\sum_{j=3} D_{ij}D_{ij} + (D_{ii})^2\right]\right\}^{(1+1/n)/2} \mathrm{d}A. \tag{4}$$

For a Newtonian rheology ($n = 1$), the quantity I defines a L^2 norm measure of the integrated in-plane deformation rates for the given flow field on the specified surface, while a power-law rheology with $n = \infty$ corresponds to the L^1 norm. It is trivial to verify that I vanishes for the Euler kinematics on the surface of a sphere, that is, no in-plane deformation is embedded within kinematics of rigid plates on the surface of the Earth. Furthermore, for the sake of comparison, the local *effective strain-rate* is defined by taking the square root of one half of the stain-rate tensor contracted with itself:

$$\dot{\epsilon}^{\mathrm{ef}} = \sqrt{\frac{(\mathbf{D}^{\mathrm{in}} : \mathbf{D}^{\mathrm{in}})}{2}}. \tag{5}$$

Once the forward calculation of the intraplate deformation for the given surface geometry and flow field is formulated, it is then possible to proceed with the implementation of a corresponding inverse problem. Inverse scheme based on such formulation has been devised (Chiao, 1993) to invert simultaneously for the optimal slab geometry and subduction flow field. In this study, however, the slab geometry is taken to be that determined from Wadati-Benioff

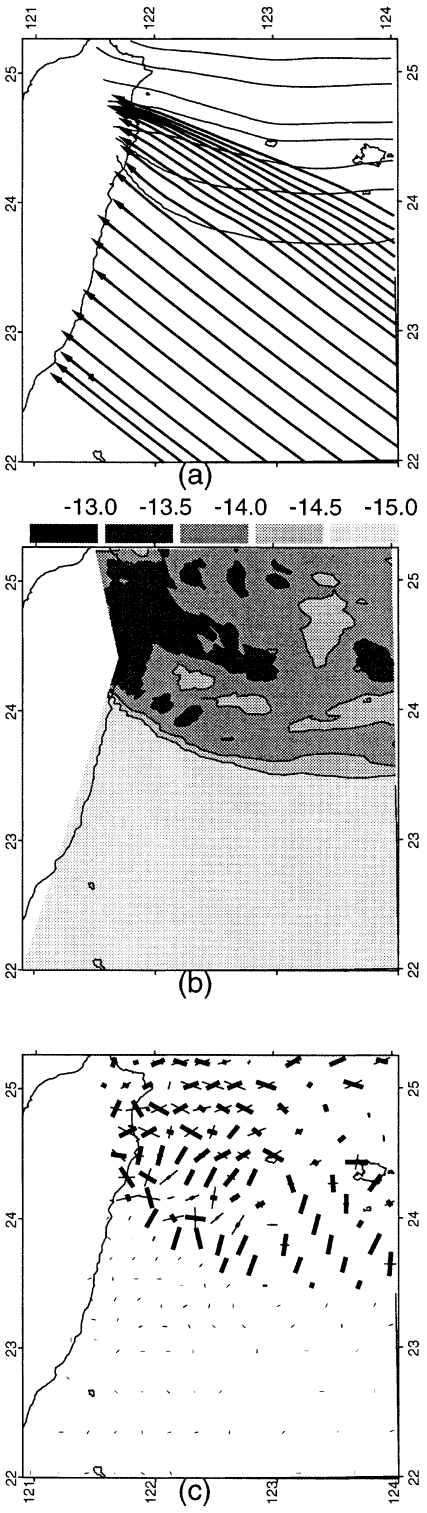

seismicity (Fig. 2; Kao et al., 1998a). The effort is thus focusing on determining the optimal flow field compromising the appropriate boundary conditions while minimizing the integrated dissipation power I defined in Eq. (4). Notice that although there has been modeling efforts incorporating dynamics such as the gravitational pulling carried on very simple ideal slab geometry (e.g. Shen, 1995), the modeling implemented in this study is strictly kinematic. In the case of the westernmost Ryukyu subduction zone, the subducted slab and the northwestern corner of PSP compose a 2D non-Euclidean surface embedded in the 3D space. The main interest of this study is concentrated on examining the potential impacts on the intraplate deformation and the possible modification of the plate kinematics set up by the slab geometry and the unfriendly collision boundary along the Longitudinal Valley suture (Fig. 2; Barrier and Angelier, 1986). The iterative scheme developed by Gill and Murray (1974) is adopted to tackle the nonlinear optimization.

3. Oblique subduction along the westernmost Ryukyu arc

Tectonic background of the modeling area (Fig. 2) portraits a complicated transition from the Ryukyu subduction to the Taiwan orogeny and to the Luzon subduction to the south (Big, 1972; Angelier, 1986). Considerable efforts of tectonics studies within this area have been paid to the crust manifestation of the orogeny on Taiwan (e.g. Suppe, 1981; Ho, 1986;

Fig. 3. Intuitive plate convergence flow field. Plate convergence prior to the subduction is determined from the Euler vectors reported by Seno et al. (1993). For the subducted Ryukyu slab, the subduction flow field ($\mathbf{V}_{REF}$ in Fig.1) is constructed by rotating the Euler vectors with respect to the local strike onto the slab surface (see the text). (a). Particle paths associated with the constructed flow field. (b). The corresponding in-plane deformation represented by the spatial pattern of the effective strain-rate (see the text). (c). The strain-rate tensor at any location is still a 3D tensor consisting the membrane deformation rate and the thickening (or thinning) of the viscous slab (Eq. (3)). Principal axes of compression (bold line segments) and extension (thin lines) of the 3D tensor are projected onto the slab surface and then projected to the surface of the Earth to reveal a map view of the in-plane strain regime. The length of bars is saturated above strain-rate of 10^{-14} s^{-1}, that is, strain-rates higher than 10^{-14} s^{-1} have the same length, and is linearly decreased for smaller strain-rates.

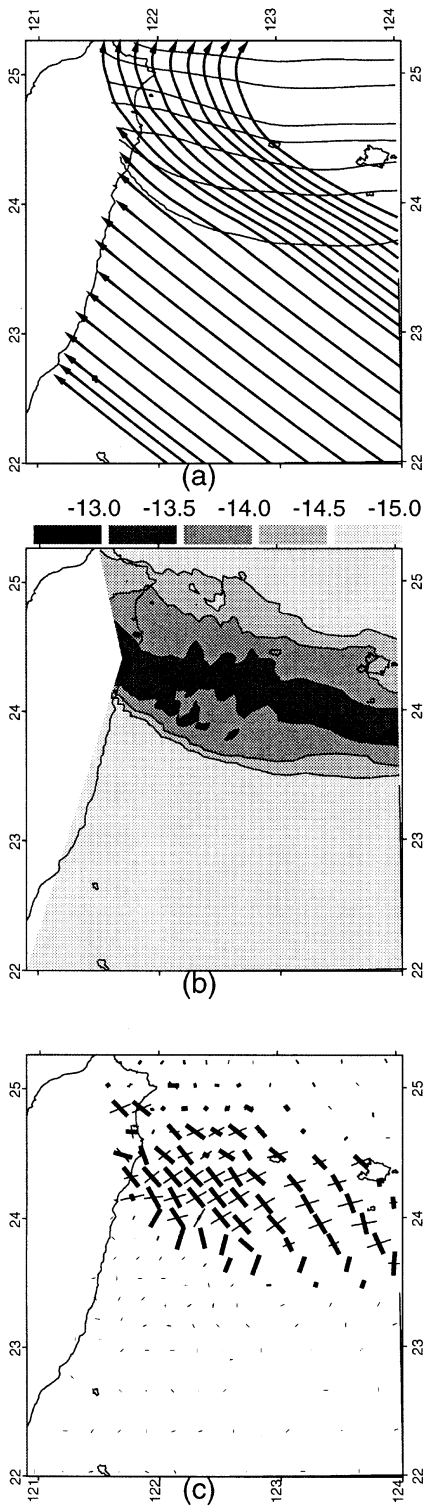

Angelier et al., 1990; Teng et al, 1992; Lu et al., 1998). Recently, polished seismotectonic characteristics of the transition from the Ryukyu subduction to the collision has been delineated (e.g. Kao et al., 1998a,b; Kao and Rau, 1999). In brief summary, there are considerable intraplate seismic activities within the northwestern corner of PSP, and the slab geometry for the westernmost subducted Ryukyu slab can be mapped by the relocated Wadati–Benioff seismicity. It is also shown that interface earthquakes within the depth range of 25–50 km are more or less clustered at a relatively small patch (marked by filled star on Fig. 2) with significant and consistent slip vector residuals. Interestingly, although there are clear transcurrent structures in the fore-arc region along the Ryukyu trench to accommodate the noted subduction obliquity in this area, no indication of the same strike–slip motion has been reported in the overriding plate near sites with slip vector residuals (Lallemand et al., 1999a,b)).

The generally accepted Euler model of the PSP–EP plate kinematics has been established by Seno et al. (1993), although it is mainly constrained by slip vectors of interface earthquakes at subduction zones far away from our modeling region. Nonetheless, we will first adopt the PSP–EP Euler pole to build an intuitive velocity field for the subducted slab with the given slab geometry of our modeling region (Fig. 2). This is done by rotating the plate convergence vectors onto the slab surface with respect to the local strike of the slab. The obliquity of plate convergence in the modeling region is shown by the particle paths delineated by this intuitive flow field (Fig. 3a). Notice that the relative displacement vectors for the subducted slab deviate slightly counterclockwise from the direction of the Euler vectors defined on the surface. This is because the subduction flow field is built by rotating, rather than radial projecting the surface Euler vectors.

We calculate $\mathbf{D}^{in}$ (Eq. 3) and the quantitative measure of the in-plane deformation I (Eq. 4) for our modeling region. The forward calculation

Fig. 4. Result of optimization experiment I. Similar to Fig.3 but for flow field constructed by minimizing the integrated in-plane deformation rate within the subducted slab (see the text and the caption of Fig. 3).

outlined in the previous section indicates that there are considerable in-plane deformations for the westernmost Ryukyu slab if the subduction follows the intuitively built velocity field (Fig. 3). Notice that the effective in-plane strain-rate (defined in Eq. (5)) amounts to about $10^{-14}\,s^{-1}$ for the entire modeled slab with peak value of $10^{-12}\,s^{-1}$near the Hualien area, where the trench is believed to intersect with the continental margin (Fig. 3b). Except near the trench, where the *P*-axes (compression axis) are more or less in the trench normal direction, the strain regime (Fig. 3c) lacks the systematic pattern revealed from observations (Kao, 1998a,b; Kao and Rau, 1999). Within our region of interest, the strain-rate field associated with the intuitive subduction flow is unrealistic, implying that an alternative optimal flow field has to be pursued.

4. Subduction flow fields that minimize the in-plane deformation

Having quantitative measures of total in-plane deformation for given surface geometry and velocity field (Eq. (4)), an inverse problem of determining the flow field that minimizes the integrated total dissipation power can be implemented. Boundary constraints are specified by assigning the flow along a spherical shell corresponding to the pure rotation of the oceanic lithosphere at southeastern corner of our modeling region, faraway from the subduction–collision transition near the northwestern corner.

4.1. Optimization modeling I

In the first optimization model, the plate convergence velocity vectors on the surface of the Earth prior to encountering the Ryukyu trench are all fixed to concord the Euler vectors reported by Seno et al. (1993). In other words, assuming that the northwestern corner of PSP is perfectly rigid, we are looking for the subduction flow field that minimizes the integrated in-plane deformation of the subducted slab. It is found after optimization that the particle paths associated with the calculated flow field (Fig. 4a) deviate significantly from the intuitive flow field (Fig. 3a). From the depth range around 30 km, the particle paths are moving toward the trench normal direction that is in better accordance with the slip vectors of interface earthquakes (Kao et al., 1998a). The spatial pattern of the effective strain-rate (Eq. (5)) shows that most of the in-plane deformation tends to concentrate in the shallower part of the slab (Fig. 4b). Clearly, the overall in-plane deformation is significantly reduced compared to Fig. 3b. Furthermore, a systematic variation of the orientation of the principal vectors of the strain-rates tensor is revealed (Fig. 4c). We find that immediately adjacent to the trench, the *P*-axes are systematically in the trench-normal direction except very close to Hualien area. To the west of 123°E and north of 24°N, the *P*-axes of the shallower portion of the slab tend to cluster in the along-strike direction of the slab surface. This seems to be consistent with the lateral compression seismogenic zone (LCSZ) reported by Kao et al. (1998a). The LCSZ has a series of intraplate earthquakes scattered in the along-strike direction with their *P*-axes systematically aligned in the along-strike direction. It has been interpreted to be closely related to the impinging of the northwestern corner of PSP with EP at the lithospheric depth range (Kao et al., 1998a). Our modeling, however, suggests that the adjustment of the subduction flow field to fit in the given slab geometry might be the dominant factor that generates the pattern of focal mechanisms within the LCSZ.

Notice that in this modeling, the potential deformation on the surface arisen from the PSP–EP collision is assumed to be concentrated on the western boundary of the modeling region, the Longitudinal Valley suture (Fig. 2). Intraplate deformation prior to subduction is assumed to be not significant. In other words, only the subduction flow field is reconfigured to minimize the in-plane deformation. Compared to the intuitive flow field, the optimized subduction flow around where the slip vectors are reported (marked by filled star in Fig. 2) turns about 12° toward the trench normal direction. This is in better accordance with the observation, but not enough to cover the observed 35° slip vector residual. The assumption of a perfectly rigid PSP prior to subduction such that flow field can be reconfigured only after subduction is, however, not rigorously founded.

4.2. Optimization modeling II

Several intriguing observations suggest that intraplate deformation occurs within the northwestern

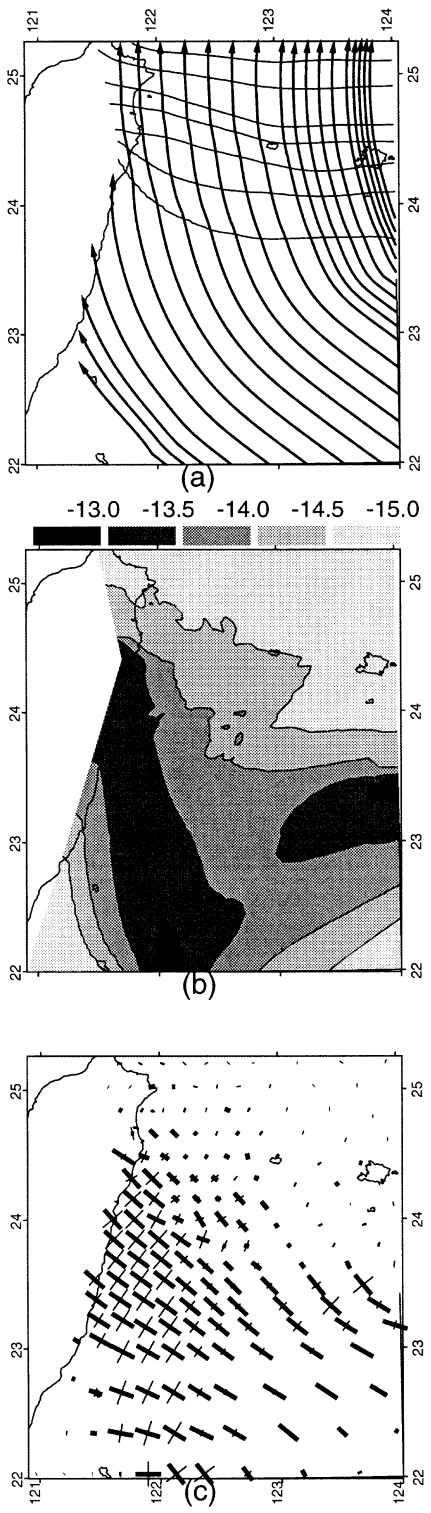

corner of PSP. Although uncommon, there are well-documented examples of intraplate deformation within the interior of oceanic plates (e.g. Denlinger, 1992). One such case is the so-called "Gorda plate", offshore of California. There, the intraplate deformation manifests into curved magnetic strips on the seafloor that are caused by discordant kinematic boundary conditions between the non-parallel Blanco fracture zone to the north and the Mendocino fracture zone to the south (Wilson, 1989; Denlinger, 1992). The discordant kinematic boundary condition is somewhat similar for the northwestern corner of PSP along the western boundary set up by the Longitudinal valley where the PSP–EP convergence is brought into collision. Unlike the Gorda plate, there are no seafloor observations that might indicate intraplate deformation. Consequently, the northwestern corner of PSP has been envisioned as a rigid indentor (e.g. Lu et al., 1998). However, a significant amount of seismic activity has been recorded to the east of the Longitudinal valley and in the offshore area that are well within the interior of PSP. Most of the focal mechanisms of these intraplate events have their *P*-axes clustered in the plate convergence direction (e.g. Kao et al., 1998a,b), indicating intraplate deformation of the northwestern corner of PSP. In addition, the *P*-axes of these intraplate earthquakes seem to reveal a gradual clockwise rotation from south to north (Angelier and Kao, 1999; Wu and Hetland, 1999). Furthermore, paleaomagnetic studies indicate a distinct clockwise rotation of the northern Coast Range relative to the south (Lee et al., 1991). Relative velocity vectors constructed from GPS measurements are also consistent with this relative rotation (Yu et al., 1990, 1997; Yu and Kuo, 1999). Wide-angle reflection/refraction data suggest distinct thickening of PSP beneath the Coastal Range (Hetland and Wu, 1998; Yang and Wang, 1998; Yeh et al., 1998) implying a possible blocking effect on the plate kinematics of PSP along the Longitudinal valley. These observations all imply that there might be intraplate deformation within the northwestern corner of PSP. Taking

Fig. 5. Result of optimization experiment II. Similar to Fig.3 but for flow field constructed by minimizing the integrated in-plane deformation rate of the complete modeling region (see the text and the caption in Fig 3).

this into consideration, we are confronted with the problem of seeking the optimized flow field representing the relative plate convergence in our modeling area on the complicated 3D surface of the northwestern corner of PSP, including the subducted slab. The most important kinematic boundary condition is that the suture along the Longitudinal valley is treated as a boundary where the plate convergence is blocked. It is worth noting that there is no intention to challenge the rigid indentor model of the Taiwan orogeny (e.g. Lu et al., 1998). It is conceivable that when the EP side of the deformation is examined, the mechanical strength of the continental lithosphere is likely to be relatively smaller than that of the oceanic lithosphere. However, if intraplate deformation within PSP is admissible, it is likely to be caused by both the geometric configuration of the obliquely subducted slab and the kinematic blocking on the western boundary.

Our second experiment is thus performed on the 3D surface of the modeling region, with kinematic boundary conditions blocked on the western side, where the longitudinal valley is located. One problem, however, is that there are no observational constraints on how severe the blocking would be, since the deformation and retreating of EP would take up some of the blocking effect. Our current scheme is to minimize the in-plane deformation of the whole modeling area and simultaneously minimize the overall integrated velocity components normal to the western boundary. Furthermore, although it is a kinematic modeling, constraint on the rheological structure is needed in the calculation. For the present calculation, a power-law rheology with $n = 10^5$ is adopted as a simple approximation toward the plastic rheology.

The result of this model reveals more drastic deviation of the particle paths with respect to the Euler vectors (Fig. 5a) and shows distinct clockwise rotation from south to north. Major deformation diffused from the collision boundary is now located within the northwestern corner of PSP on the surface instead of the subducted slab. Interestingly, the area with higher deformation rate is not concentrated along the Longitudinal valley but seems to coincide with the previously reported collision seismogenic zone (CSZ) (Kao et al., 1998a) near Taiwan (Fig. 5b). The resulted systematic pattern of *P*-axes orientation is consistent with seismic observations (Fig. 5c).

5. Conclusions and discussion

The idea of allowing intraplate deformation within the northwestern corner of PSP and the westernmost subducted Ryukyu slab, and thus modifies the local plate convergence kinematics, was explored in this study and provides useful insights in interpreting geophysical observations in this area. Different scenarios of the plausible flow field of the local plate kinematics are compared in perspective (Fig. 6). Although intuitively rotating Euler vectors onto the slab surface (Fig. 6a) seems to be generally adopted, the merit of such conventional practice in terms of having non-yielding oceanic lithosphere is unwarranted. In the optimization model I, the subduction flow field trying to fit in the slab geometry will have to be reconfigured to significantly reduce the in-plane deformation. In other words, the modification of particle paths (compare Fig. 6b with 6a) is a natural consequence of minimizing the integrated in-plane deformation rate. In the optimization model II, the PSP–EP convergence is blocked along the collision boundary, in addition to the geometric constraint considered in model I. Assuming that the deformation arisen from collision is not confined within the suture, gradual distortion of the northwestern corner of PSP will endure significantly less deformation by deviating the flow field even further away from the Euler kinematics (Fig. 6c). Both results from these experiments are suggesting that the slip vector residuals observed in this area might not be as large as those measured with respect to the conventional reference.

Although the two experiments adopt viscous power-law rheology and thus favor the gradual creeping as the deformation mechanism, the possibility that deformation may take place discretely along concentrated shear zones is not excluded. In fact, with suitable rheology, the high deformation rates distribution in Fig. 3b can also be interpreted as a roughly E–W trending diffuse shear zone or a major tear fault within the subducted slab (Lallemand et al., 1999a). Both of these interpretations imply the reconfiguration of the subduction flow field or "strain partitioning within the subducted slab" (Lallemand et al., 1999a). It is presently not feasible to differentiate these two very different interpretations from seismotectonic data. Nonetheless, it is worth emphasizing again, that be it the gradual creeping or the discretely concentrated

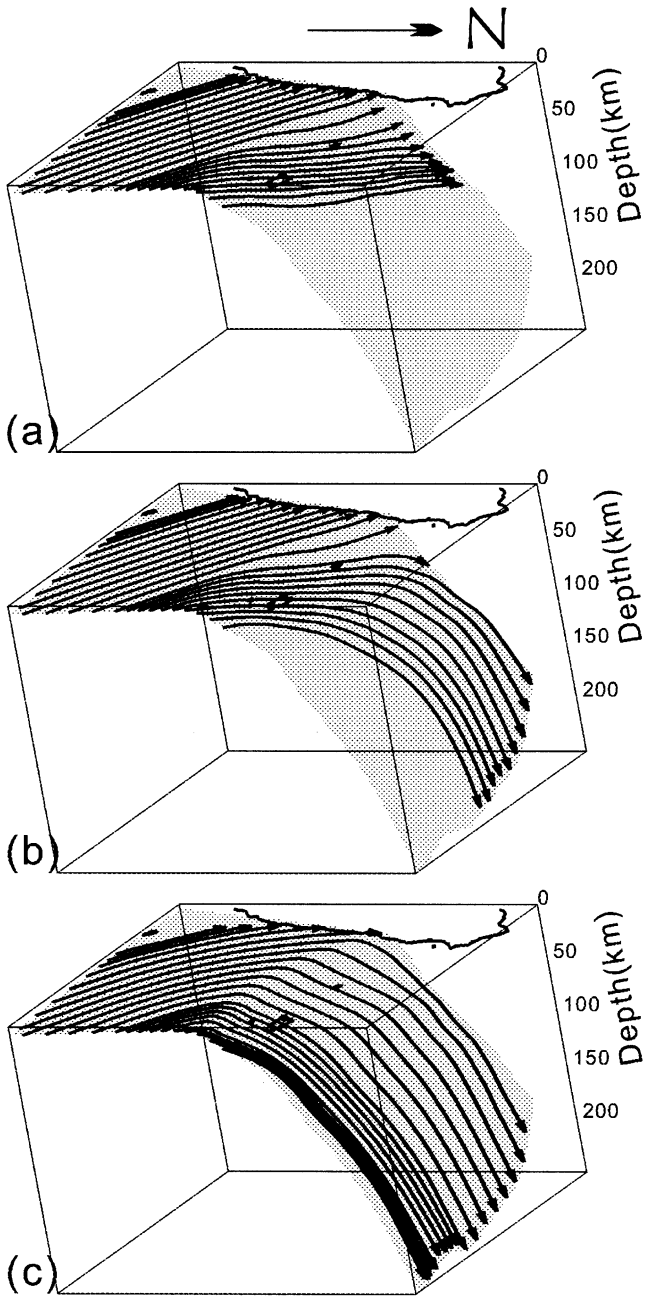

Fig. 6. 3D perspective plots of the particle paths of different scenarios discussed in this study (see discussions in the text). (a). Case I: Intuitive flow field by rotating Euler vectors onto the slab surface. (b). Case II (optimization experiment I): flow field minimizing the integrated in-plane deformation rate of the subducted slab. (c). Case III (optimization experiment II): flow field minimizing the overall in-plane deformation rate in the entire modeling region. Notice the significant clockwise rotation of particle paths portrayed in (b) and (c) as compared to (a).

shearing, the inevitable end effect will be the significant clockwise rotation of the subduction flow field.

There are thus two important concepts that we wish to raise for the tectonic studies of our modeling area. The first is that the westernmost Ryukyu slab and the northwestern corner of PSP are not two separate tectonic units but a coherent, continuous system. Secondly, the possibility of considerable intraplate deformation within this system may be responsible for significant reconfiguration of the local plate kinematics (Fig. 6b and c). The rationale does not violate the theory of plate tectonics. Under "unfriendly" geometric and kinematic boundary constraints that enforce intraplate deformation, it is conceivable that one way to respect the mechanical strength of the oceanic lithosphere is to reconfigure the relative plate convergence velocity field such that the oceanic lithosphere endures the minimum in-plane deformation. Plate kinematics calculated in this area based on such a principle seems to offer more compatible tectonic interpretations of geophysical observations.

However, there are at least three factors that will affect our calculations: (1) the precise slab geometry of the westernmost Ryukyu slab; (2) a realistic rheological structure; and (3) the degree of blocking along the Longitudinal valley suture. In this study, we assumed that the slab geometry is reliably determined by relocated slab seismicity (Kao et al., 1998a). Refinements on the slab geometry, especially beneath northeastern Taiwan where the pronounced subduction obliquity is taking place, needs to be undertaken. In fact, the exact configuration of the trench, which is the pivot axis of the subduction, is still loosely constrained for the segment west of the Gagua ridge (roughly along 123°E), especially near the intersection with the island of Taiwan, and needs to be clearly determined.

Also, we have adopted a high power-law rheology ($n = 10^5$ in Eq. (4)) as a crude approximation to carry a L^1 norm minimization. The essence of this strategy is simply trying to concentrate the in-plane deformation where it is necessary, as opposed to a Newtonian flow ($n = 1$) that will distribute the deformation throughout the modeling region. Although the L^1 norm versus L^2 norm choice seems reasonable, more realistic long-term rheological behavior of the oceanic lithosphere needs to be considered to devise more robust calculation (e.g. Denlinger, 1992). Previous discussion concerning the deformation regime from gradual creeping to concentrated shearing within the slab, is a dispute on the rheological structure. Similarly, although gradual distortion close to the plate boundary is proposed within the northwestern corner of PSP on the surface from the optimization model II, a similar scenario of having series of concentrated NEE–SWW trending shear zones to the north close to the Ryukyu trench and NNW–SSE shear zones within the CSZ to the southwest, close to Taiwan, are also possible. The scenario suggested in Fig.5 can probably be treated as an upper limit of the possible clockwise rotation. Furthermore, considering the lateral heterogeneity of the mechanical strength within PSP and the degree of blocking along the Longitudinal valley suture, the intraplate deformation may be entrenched to the west of the Luzon arc (Fig. 2) as the distribution of seismicity seems to suggest. In other words, the actual deformation regime and the plate kinematics flow field are very likely in between our results of modeling I and modeling II.

Acknowledgements

We benefit significantly from the intriguing atmosphere created within the ROC–France cooperation frame in Earth Sciences supported by the National Science Council (NSC) and the Institut Francais a Taipei. Review comments from Prof. Jacques Angelier and another anonymous reviewer as well as the editor have improved both the scientific reasoning and the presentation greatly. Some of the figures of this article are generated using the GMT package of Wessel and Smith. This research was supported by NSC under grant NSC 88-2611-M-002-023.

References

Angelier, J., 1986. Geodynamics of the Eurasia–Philippine Sea plate boundary: Preface. Tectonophysics 125, LX–X.

Angelier, J., Bergerat, F., Chu, H.-T., Lee, T.-Q., 1990. Tectonic analysis and the evolution of a curved collision belt: the Hsueh-shan Range, northern Taiwan. Tectonophysics 183, 77–96.

Angelier, J., Kao, H. 1999. Inversion of focal mechanisms of relocated earthquakes and regional seismotectonic fields in and around Taiwan, extended abstract, 4th France–Taiwan Symposium, Montpellier, pp. 203–206.

Barrier, E., Angelier, J., 1986. Active collision in eastern Taiwan: the Coast Range. Tectonophysics 125, 9–72.

Big, C., 1972. Dual-trench structure in the Taiwan–Luzon region. Proc. Geol. Soc. China 15, 65–75.

Burback, G.V., Frolich, C., 1986. Intermediate and deep seismicity and lateral structure of subducted lithosphere in the circum-Pacific region. Rev. Geophys. Space Phys. 24, 833–874.

Chiao, L.-Y., 1993. Strain segmentation and lateral membrane deformation rate of the subducted Ryukyu slab. The Island Arc 2, 94–103.

Creager, K.C., Boyd, T.M., 1991. The geometry of Aleutian subduction: three-dimensional kinematic flow modeling. J. Geophys. Res. 96, 2293–2307.

Denlinger, R.P., 1992. A model for large-scale plastic yield of the Gorda deformation zone. J. Geophys. Res. 97, 15 415–15 423.

Fitch, T.J., 1972. Plate convergence, transcurrent fault, and internal deformation adjacent to southeast Asia and the Western Pacific. J. Geophys. Res. 77, 4432–4460.

Gill, P.E., Murray, W., 1974. Newton-type methods for unconstrained and linearly constrained optimization. Math. Progm. 7, 311–350.

Hetland, E., Wu, F.T., 1998. Deformation of the Philippine Sea plate under the Coastal Range, Taiwan: Results from an offshore–onshore seismic experiment. TAO 9, 363–378.

Ho, C.-S., 1986. A synthesis of the geological evolution of Taiwan. Tectonophysics 125, 1–26.

Kao, H., Shen, S.J., Ma, K.-F., 1998a. Transition from oblique subduction to collision: Earthquakes in the southernmost Ryukyu arc–Taiwan region. J. Geophys. Res. 103, 7211–7229.

Kao, H., Jian, P.-R., Ma, K.-F., Huang, B.-S., Liu, C.-S., 1998b. Moment-tensor inversion for offshore earthquakes east of Taiwan and their implications to regional collision. Geophys. Res. Lett. 25, 3619–3622.

Kao, H., Rau, R.-J., 1999. Detailed structures of the subducted Philippine sea plate beneath northeast Taiwan: a new type of double seismic zone. J. Geophys. Res. 104, 1015–1033.

Lallemand, S., Kao, H., Font, Y., Liu, C.-S., 1999. Strain partitioning within a subducting plate? The case of the southern Ryukyu subduction zone, extended abstract, 4th France–Taiwan Symposium, pp. 53–57.

A.C.T. Scientific Crew, Lallemand, S., Liu, C.-S., Dominguez, S., Schnurle, P., Malavieille, J., 1999b. Scientific Crew, Trench-parallel stretching and folding of forearc basins and lateral migration of the accretionary wedge in the southern Ryukyus: a case of strain partition caused by oblique convergence. Tectonics 18, 231–247.

Lee, T.Q., Kissel, C., Barrier, E., Laj, C., Chi, W.R., 1991. Paleomagnetic evidence for a diachronic clockwise rotation of the Coastal Range, eastern Taiwan. Earth Planet. Sci. Lett. 104, 245–257.

Liu, X.-P., McNally, K.C., Shen, Z.-K., 1995. Evidence for a role of downgoing slab in earthquakes slip partitioning at oblique subduction zones. J. Geophys. Res. 100, 15 351–15 372.

Lu, C.-Y., Yu, S.-B., Chu, H.-T., 1998. Neotectonics of the Taiwan mountain belt. In: Flower, M.F.J., Chung, S.-L., Lo, C.-H., Lee, T.-Y., Uyeda, S. (Eds.). Mantle dynamics and plate interaction in East Asia. AGU Geodyn., 27, pp. 301–315.

McCaffrey, R., 1992. Oblique plate convergence, slip vectors, and forearc deformation. J. Geophys. Res. 97, 8905–8915.

McCaffrey, R., 1993. On the role of the upper plate in great subduction zone earthquakes. J. Geophys. Res. 98, 11 953–11 966.

McCaffrey, R., 1994. Global variability in subduction thrust zone-forearc system. Pure Appl. Geophys. 142, 174–224.

Seno, T., Stein, S., Gripp, A.E., 1993. A model for the motion of the Philippine Sea plate consistent with NUVEL-1 and geological data. J. Geophys. Res. 98, 17 941–17 948.

Shen, Z.-K., 1995. Oblique subduction of a Newtonian fluid slab. Pure Appl. Geophys. 145, 561–577.

Suppe, J., 1981. Mechanics of mountain building and metamorphism in Taiwan. Mem. Geol. Soc. China 4, 67–89.

Teng, L., Chen, C.-H., Wang, W.-S., Liu, T.-K., Juang, W.-S., Chen, J.-C., 1992. Plate kinematic model for late Cenozoic arc magmatism in northern Taiwan. J. Geol. Soc. China 36, 1–18.

Wilson, D.S., 1989. Deformation of the so-called Gorda plate. J. Geophys. Res. 94, 3065–3075.

Wu, F.T., Hetland, E., 1999. Focal mechanisms of earthquakes offshore of eastern Taiwan and intraplate deformation, abstract, 4th France–Taiwan Symposium, Montpellier, pp. 207.

Yamaoka, K., Fuako, Y., Kumazawa, M., 1986. Spherical shell tectonics: Effects of sphericity and inextensibility on the geometry of the descending lithosphere. Rev. Geophys. 24, 27–55.

Yang, Y.-S., Wang, T.-K., 1998. Crustal variation of the western Philippine Sea plate from TAICRUST MCS/OBS line 23. TAO 9, 379–394.

Yeh, Y.-H., Shih, R.-C., Lin, C-H., Liu, C.-C., Yen, H.-Y., Huang, B.-S., Liu, C.-S., Wu, F.T., 1998. Onshore/offshore wide-angle deep seismic profiling in Taiwan. TAO 9, 301–316.

Yu, S.-B., Jackson, D.D., Yu, G.-K., Liu, C.-C., 1990. Dislocation model for crustal deformation in the Longitudinal Valley, eastern Taiwan. Tectonophysics 183, 97–109.

Yu, S.-B., Chen, H.-Y., Kuo, L.-C., 1997. Velocity field of GPS stations in the Taiwan area. Tectonophysics 274, 41–59.

Yu, S.-B., Kuo, L.-C., 199. GPS observation of crustal deformation in the Taiwan-Luzon region. Geophys. Res. Lett. 26, 923–926.